



Four novel isostructural coordination polymers $\{[M(H'L)_2(H_2O)_2] \cdot 2DMF\}$ [$M = Zn(II), Cd(II), Mn(II)$ and $Co(II)$] built using a nitrogen and oxygen donor azo ligand: Crystal structures and fluorescence studies

Rupali Mishra^a, Musheer Ahmad^b, Madhav Ram Tripathi^{a,*}

^a Department of Chemistry, D.A.V. College, C.S.J.M. University, Kanpur 208001, India

^b Department of Chemistry, Indian Institute of Technology Kanpur, Kanpur 208016, India

ARTICLE INFO

Article history:

Received 16 January 2013

Accepted 9 February 2013

Available online 27 February 2013

Keywords:

Coordination polymer

Transition metal ions

X-ray structural studies

Crystal structure

Thermogravimetric analyses (TGA)

Photoluminescence studies

ABSTRACT

When the ligand $HH'L$ was treated with different transition metal salts at room temperature, four new isostructural coordination polymers, $\{[Zn(H'L)_2(H_2O)_2] \cdot 2DMF\}_n$ (**1**), $\{[Cd(H'L)_2(H_2O)_2] \cdot 2DMF\}_n$ (**2**), $\{[Mn(H'L)_2(H_2O)_2] \cdot 2DMF\}_n$ (**3**), and $\{[Co(H'L)_2(H_2O)_2] \cdot 2DMF\}_n$ (**4**) ($HH'L = 2$ -hydroxy-5-(pyridin-4-ylazo)-benzoic acid) were formed. These polymers were characterized by IR spectroscopy, elemental analysis, powder X-ray diffraction (PXRD) and thermogravimetric analysis (TGA), in addition to X-ray crystallography. X-ray single crystal studies revealed that **1–4** are 1D coordination polymers that are further extended by weak interactions to afford 3D coordination polymers. All the complexes show high thermal stability after losing coordinated and lattice solvent molecules in the temperature range 80–200 °C. Upon excitation at 344 nm, complexes **1–4** exhibit solid-state luminescence at room temperature.

© 2013 Elsevier Ltd. All rights reserved.

1. Introduction

Recent years have witnessed an immense growth in the field of coordination polymers (CPs) for their potential applications in gas adsorption [1–3], molecular storage [4,5], catalysis [6–8], proton conductivity [9], magnetism [10–13], luminescence [14–16], drug delivery [17,18] and so on. Specifically, controlled design to accommodate small molecules that can be further assembled into supramolecular entities is one of the promising areas of increasing interest in recent years [19]. Usually the intriguing topologies of coordination polymers can be controlled by proper design and characteristic features of the ligands, like rigidity, flexibility, bulkiness and so on [20]. Since the incorporation of well-organized structural motifs into a crystal lattice may generate novel materials with engineered physical and chemical features, such work can give an insight into the molecular assemblies and their functions. Additionally, the tendency of metal ions to adopt certain geometries and the prevailing experimental conditions, counter-anions, temperature, solvents, pH and so on, have considerable influence on the overall structure of the frameworks [21]. Besides the above factors, the crystallization conditions play a crucial role in the self-assembly processes.

Most researchers pay attention to design and exploit symmetric cylindrical or bridging organic ligands for the construction of coordination polymers [22]. However, unsymmetrical ligands having different denticities with different donors can assemble metal centers to give rise to a large number of coordination polymers. Ligands having both nitrogen [23] and carboxylate [24–27] donors have been used extensively for this purpose. Motivated by this, we have designed the ligand, 2-hydroxy-5-(pyridin-4-ylazo)-benzoic acid, with an azo moiety in the middle as shown in the Scheme 1. This design provides a certain degree of conformational freedom around the azo moiety that may lead to CPs with different overall architectures.

Herein, we report the synthesis and crystal structural studies of four coordination polymers, $\{[Zn(H'L)_2(H_2O)_2] \cdot 2DMF\}_n$ (**1**), $\{[Cd(H'L)_2(H_2O)_2] \cdot 2DMF\}_n$ (**2**), $\{[Mn(H'L)_2(H_2O)_2] \cdot 2DMF\}_n$ (**3**), and $\{[Co(H'L)_2(H_2O)_2] \cdot 2DMF\}_n$ (**4**). These compounds have also been subjected to different physico-chemical studies, including solid-state photoluminescence.

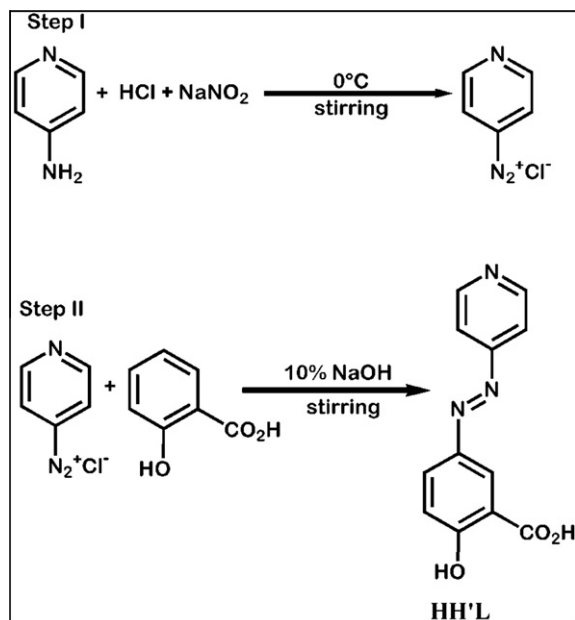
2. Experimental

2.1. General methods and materials

4-Aminopyridine, salicylic acid, $Zn(ClO_4)_2 \cdot 6H_2O$, $Cd(NO_3)_2 \cdot 4H_2O$, $MnSO_4 \cdot H_2O$ and $CoCl_2 \cdot 6H_2O$ were purchased from Aldrich, USA and were used as received. Hydrochloric acid, sodium hydroxide

* Corresponding author. Tel.: +91 512 2306687; fax: +91 512 2304534.

E-mail address: madhavamtripathi@gmail.com (M.R. Tripathi).



Scheme 1. Synthetic reaction scheme of HH'L.

pellets, NaNO₂ and solvents were procured from S. D. Fine Chemicals, India. All the solvents were purified prior to use following standard methods.

Infrared spectra were recorded on a Perkin-Elmer Model 1320 spectrometer (KBr disk, 400–4000 cm⁻¹). ¹H NMR and ¹³C NMR spectra were recorded on a JEOL-ECX 500 FT (500 and 125 MHz, respectively) instrument in DMSO-*d*₆ with Me₄Si as the internal standard. ESI-mass spectra were recorded on a WATERS Q-TOF Premier mass spectrometer. Thermogravimetric analyses (TGA) were recorded on a Mettler Toledo Star System (heating rate of 5 °C/min). Microanalyses for the compounds were obtained using a CE-440 elemental analyzer (Exeter Analytical Inc.). Solid-state photo-excitation and emission spectra were recorded using a double UV-Vis spectrophotometer (Shimadzu, UV-2450) and a Jobin Yvon Horiba Fluorolog-3 spectrofluorimeter at room temperature. Powder X-ray diffraction (Cu Kα radiation, scan rate 3°/min, 293 K) was performed on a Bruker D8 Advance Series 2 powder X-ray diffractometer.

2.2. Synthesis

2.2.1. Synthesis of 2-hydroxy-5-(pyridin-4-ylazo)-benzoic acid (HH'L)

The ligand was synthesized following an earlier reported [28] procedure with a slight modification. 4-Aminopyridine (5.06 g, 53.8 mmol) was mixed with HCl (16 mL) and digested in a water bath for 50 min. The hydrochloride was cooled to 5 °C and diazotized with ice-cold aqueous NaNO₂ (3.7 g, 20 mL). A cold solution of salicylic acid (7.42 g, 53.8 mmol), previously dissolved in 10% NaOH solution (50 mL), was then added to the cold solution of the diazonium salt solution with vigorous stirring. An orange color developed almost immediately and the stirring was continued for 1 h. The reaction mixture was kept overnight in a refrigerator, followed by 5 h at room temperature and then poured into water, whereupon an orange colored product precipitated out. The precipitate was filtered, washed several times with water and air-dried. The crude product was recrystallized from methanol to yield pure HH'L (4.72 g, 36%). ¹H NMR (DMSO-*d*₆), δ (ppm): 8.77 (Ar, 2H), 8.3 (ArH, 1H), 8.05 (ArH, 2H), 7.47 (Ar, 1H), 7.08 (ArH, 1H), due to moisture both the acid and hydroxyl protons mutually exchanged. ¹³C NMR (DMSO-*d*₆), δ (ppm): 114.2, 117.6, 119.7, 130.8, 136.2, 150.4, 161.6, 162.6, 172.5. Elemental analysis: *Anal. Calc.* for C₁₂H₉N₃O₃ (243.2211): C, 59.26; H, 3.73; N, 17.27. Found: C, 59.38; H, 3.62; N, 17.12%. ESI-MS *m/z*: 244.0727 [M+1]⁺.

2.2.2. Synthesis of {[Zn(H'L)₂(H₂O)₂]·2DMF}_n (1)

A hot DMF solution (3 mL) of the ligand HH'L (0.039 g, 0.16 mmol) was added to a MeOH/H₂O solution (1:1, 2 mL) of Zn(ClO₄)₂·6H₂O (0.059 g, 0.16 mmol). On slow evaporation of the filtrate at RT, orange crystals of **1** were obtained in ~80% Yield. *Anal. Calc.* for C₃₀H₃₄N₈O₁₀Zn: C, 49.22; H, 4.68; N, 15.31. Found: C, 49.34; H, 4.78; N, 15.22%. IR (KBr, cm⁻¹): 3205(s), 2929(w), 1666(s), 1620(m), 1602(m), 1483(m), 1461(s), 1435(s), 1384(m), 1352(m), 1272(w), 1166(s), 1074(m), 840(s), 811(m), 784(m), 691(m).

2.2.3. Synthesis of {[Cd(H'L)₂(H₂O)₂]·2DMF}_n (2)

A mixture of Cd(NO₃)₂·4H₂O (0.062 g, 0.2 mmol) and HH'L (0.049 g, 0.2 mmol) was dissolved in DMF/EtOH/H₂O solution (6 mL, 1.5:1:1 v/v), and the mixture was stirred for 2 h at room temperature, then filtered. On slow evaporation of the filtrate, orange block shaped crystals of **2** were obtained in ~48% yield. The crystals were repeatedly washed with EtOH and dried in air. *Anal.*

Table 1
Crystal and structure refinement data for 1–4.

Compound	1	2	3	4
Formula	C ₃₀ H ₃₄ N ₈ O ₁₀ Zn	C ₃₀ H ₃₄ N ₈ O ₁₀ Cd	C ₃₀ H ₃₀ N ₈ O ₁₀ Mn	C ₃₀ H ₃₄ N ₈ O ₁₀ Co
Formula weight	732.02	779.05	717.56	725.58
<i>T</i> (K)	100(2)	100(2)	100(2)	100(2)
System	monoclinic	monoclinic	monoclinic	monoclinic
Space group	C2/c	C2/c	C2/c	C2/c
<i>a</i> Å	18.151(5)	18.423(5)	18.319(5)	18.170(5)
<i>b</i> Å	11.169(5)	11.190(7)	11.066(5)	11.067(5)
<i>c</i> Å	18.400(5)	18.324(5)	18.528(5)	18.487(5)
α (°)	90.000	90.000	90.000	90.000
β (°)	118.825(5)	118.351(4)	118.619(5)	118.954(5)
γ (°)	90.000	90.000	90.000	90.000
<i>V</i> [Å ³]	3268.0(19)	3324(2)	3297(2)	3252.7(19)
<i>Z</i>	4	4	4	4
ρ _{calc} [g/cm ³]	1.488	1.557	1.446	1.482
μ [mm ⁻¹]	0.821	0.725	0.469	0.597
<i>F</i> (000)	1520	1592	1484	1508
Goodness-of-fit	1.035	1.131	1.091	1.036
Final <i>R</i> indices [<i>I</i> > 2σ(<i>I</i>)]	<i>R</i> ₁ = 0.0557, <i>WR</i> ₂ = 0.1461	<i>R</i> ₁ = 0.0417, <i>WR</i> ₂ = 0.1046	<i>R</i> ₁ = 0.0634, <i>WR</i> ₂ = 0.1732	<i>R</i> ₁ = 0.0616, <i>WR</i> ₂ = 0.1578
<i>R</i> indices (all data)	<i>R</i> ₁ = 0.0713, <i>WR</i> ₂ = 0.1626	<i>R</i> ₁ = 0.0479, <i>WR</i> ₂ = 0.1196	<i>R</i> ₁ = 0.0856, <i>WR</i> ₂ = 0.2058	<i>R</i> ₁ = 0.0822, <i>WR</i> ₂ = 0.1732
CCDC number	890674	890675	890676	890677

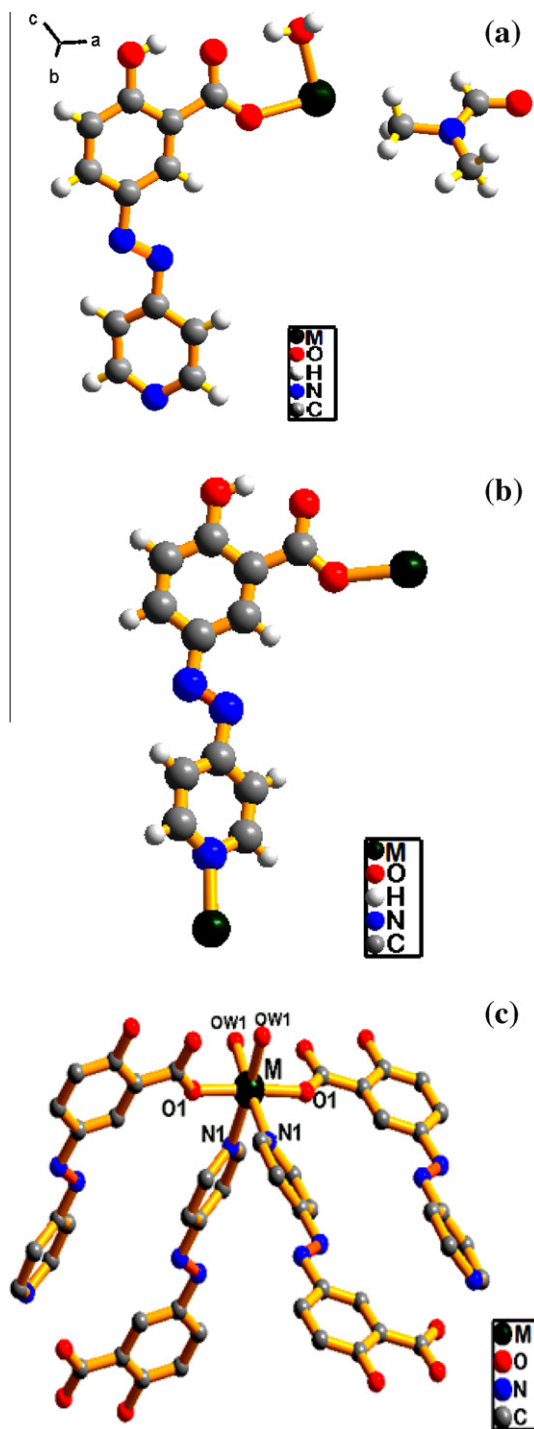


Fig. 1. Diagram showing (a) the asymmetric unit, (b) the coordination modes of the ligand $\text{H}'\text{L}^{-1}$ and (c) the coordination modes of the $\text{M}(\text{II})$ ions.

Calc. $\text{C}_{30}\text{H}_{34}\text{N}_8\text{O}_{10}\text{Cd}$: C, 46.25; H, 4.39; N, 14.38. Found: C, 46.13; H, 4.46; N, 14.27%. IR (KBr, cm^{-1}): 3395(s), 2928(w), 1667(m), 1599(s), 1464(s), 1416(s), 1385(s), 1296(w), 1165(s), 1098(m), 1073(m), 1012(m), 832(w), 810(s), 692(w).

2.2.4. Synthesis of $\{[\text{Mn}(\text{H}'\text{L})_2(\text{H}_2\text{O})_2] \cdot 2\text{DMF}\}_n$ (**3**)

A mixture of $\text{MnSO}_4 \cdot \text{H}_2\text{O}$ (0.084 g, 0.5 mmol) and $\text{HH}'\text{L}$ (0.097 g, 0.4 mmol) was dissolved in DMF/ H_2O solution (6 mL, 2:1 v/v), and the mixture was then stirred for 10 h at room temperature. The resulting solution was filtered and allowed to cool to room temper-

ature; red colored crystals of **3** were obtained in ~52% yield. The crystals were filtered, washed with acetone and dried in air. *Anal.* Calc. for **3**, $\text{C}_{30}\text{H}_{34}\text{N}_8\text{O}_{10}\text{Mn}$: C, 50.21; H, 4.21; N, 15.61. Found: C, 49.72; H, 4.93; N, 15.42%. IR (KBr, cm^{-1}): 3265(s), 2922(w), 1668(s), 1610(s), 1593(s), 1460(s), 1383(s), 1352(s), 1294(m), 1273(m), 1167(s), 1099(m), 1075(m), 934(w), 891(w), 839(s), 811(s), 666(m).

2.2.5. Synthesis of $\{[\text{Co}(\text{H}'\text{L})_2(\text{H}_2\text{O})_2] \cdot 2\text{DMF}\}_n$ (**4**)

A mixture of $\text{CoCl}_2 \cdot 6\text{H}_2\text{O}$ (0.059 g, 0.25 mmol) and $\text{HH}'\text{L}$ (0.073 g, 0.3 mmol) was dissolved in DMF/MeOH/ H_2O (3 mL, 1:1:1 v/v). The above solution was stirred for 10 h at room temperature. After filtration, the filtrate was kept at room temperature for slow evaporation. Dark orange colored crystals of **4** were obtained in ~62% yield. The crystals were filtered, washed with acetone and dried in air. *Anal.* Calc. for **4**, $\text{C}_{30}\text{H}_{34}\text{N}_8\text{O}_{10}\text{Co}$: C, 49.66; H, 4.72; N, 15.44. Found: C, 49.58; H, 4.60; N, 15.32%. IR (KBr, cm^{-1}): 3253(s), 2930(w), 1667(s), 1620(s), 1435(s), 1384(m), 1353(s), 1166(s), 1098(m), 1074(m), 967(w), 840(s), 811(m), 691(m), 580(s).

2.3. X-ray structural studies

Single crystal X-ray data of complexes **1–4** were collected at 100 K on a Bruker SMART APEX CCD diffractometer using graphite monochromated Mo $\text{K}\alpha$ radiation ($\lambda = 0.71073 \text{ \AA}$). The linear absorption coefficients, scattering factors for the atoms and anomalous dispersion corrections were taken from the International Tables for X-ray Crystallography [29]. The data integration and reduction were carried out with SAINT [30] software. An empirical absorption correction was applied to the collected reflections with SADABS [31] and the space group was determined using XPREP [32]. The structures were solved by direct methods using SHELXTL-97 [33] and refined on F^2 by full-matrix least-squares using the SHELXL-97 [34] program package. The H atoms were refined as follows; the hydrogen atoms attached to carbon atoms were positioned geometrically and treated as riding atoms using SHELXL default parameters. The H atoms of the coordinated water molecule in complex **3** could not be fixed using refinement with the DFIX command, while in the cases of **1**, **2** and **4** the H atoms of coordinated water molecules were located from difference Fourier maps. So, the H-bonding parameters in complex **3** due to the coordinated aqua hydrogen could not be located. The crystal and refinement data are collected in Table 1.

3. Results and discussion

Complexes **1–4**, once isolated, were found to be air-stable and slightly soluble in DMF, but insoluble in other common organic solvents or water. The IR spectra of **1–4** show strong absorption bands between 1414 and 1620 cm^{-1} , attributable to coordinated carboxylate groups.¹ The broad peak centered in the region 3205–3395 cm^{-1} indicates the presence of coordinated water molecules [35]. The sharp stretching frequency at $\sim 1667 \text{ cm}^{-1}$ is the signature of the carbonyl group of lattice DMF molecules.

3.1. Structural description

Single-crystal X-ray determination at 100 K reveals that complexes **1–4** are isostructural. Interestingly, all the structures were successfully solved and converged in the monoclinic space group C2/c . Here we describe the structure **1** only. The asymmetric unit of **1** contains one Zn(II) ion with half occupancy, one ligand unit

¹ See Supporting information.

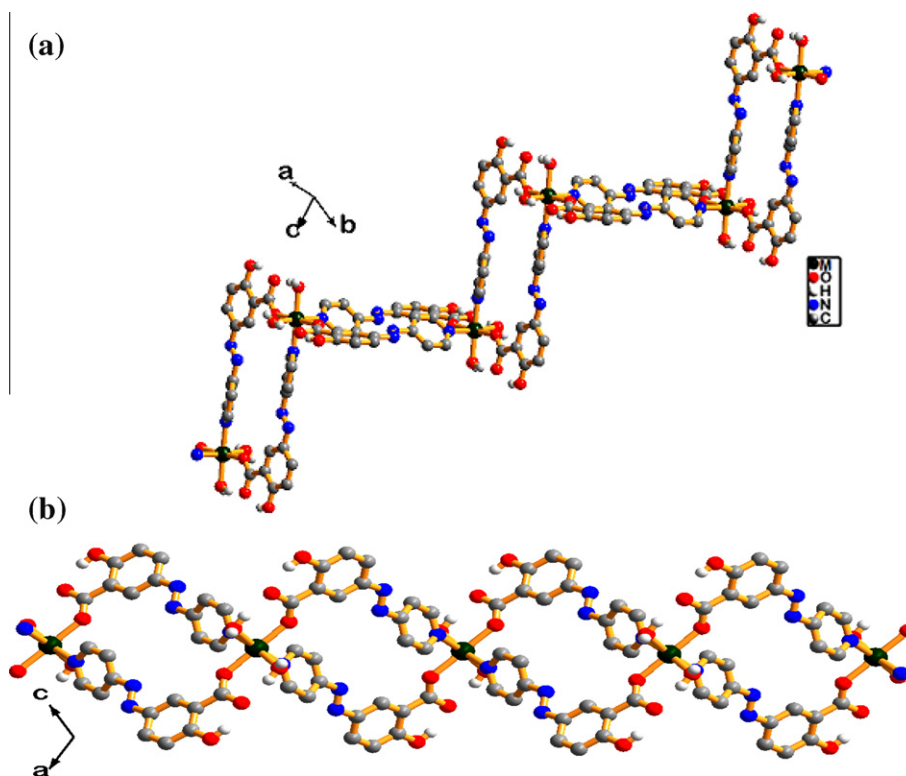


Fig. 2. 1D view of the coordination polymers (a) running along the crystallographic *bc* plane and (b) the chain propagating along the crystallographic *b*-axis.

Table 2
Selected bond distances (Å) and bond angles (°) for **1–4**.

Compound	Bond distances (Å)	Bond angles (°)
Complex 1	Zn1 O1 W = 2.089(3)	O1 W Zn1 N1 = 88.40(14)
	Zn1 N1 = 2.164(3)	O1 W Zn1 O1 = 87.71(12)
	Zn1 O1 = 2.127(3)	O1 Zn1 N1 = 85.45(11)
Complex 2	Cd1 OW1 = 2.278(3)	OW1 Cd1 N1 = 87.12(11)
	Cd1 N1 = 2.343(3)	OW1 Cd1 O1 = 85.36(9)
	Cd1 O1 = 2.291(3)	O1 Cd1 N1 = 91.90(10)
Complex 3	Mn1 OW1 = 2.175(3)	OW1 Mn1 N1 = 88.45(11)
	Mn1 N3 = 2.271(3)	OW1 Mn1 O1 = 85.86(9)
	Mn1 O1 = 2.180(3)	O1 Mn1 N1 = 91.89(10)
Complex 4	Co1 O5 = 2.088(3)	O5 Co1 N1 = 88.63(13)
	Co1 N1 = 2.148(3)	O5 Co1 O1 = 87.71(12)
	Co1 O1 = 2.114(3)	O1 Co1 N1 = 91.71(11)

Table 3
Selected hydrogen bond distances (Å) and bond angles (°) in **1–4**.

Compound	Donor–H...acceptor	D–H	H...A	D...A	D–H...A
Complex 1	O1W–H1W...O4	0.62 (5)	2.09 (5)	2.686(5)	161
	O1W–H2W...O2	0.88 (8)	1.85 (8)	2.676(5)	155
	O3–H1W1...O2	0.82	1.80 (3)	2.533(5)	148
Complex 2	O1W–H1W1...O2	0.93 (4)	1.88 (4)	2.686(5)	143
	O1W–H2W1...O3	0.96 (4)	1.82 (5)	2.674(5)	147
	O(4)–H(3)...O	0.82	1.81 (2)	2.537 (3)	147
Complex 3	O(3)–H(3)...O	0.82	1.80 (4)	2.529(5)	148
Complex 4	O(5)–H1W1...O	0.86 (8)	1.84 (8)	2.672(5)	162
	O(5)–H2W1...O	0.6 (6)	2.07 (6)	2.693(5)	157
	O(3)–H(3)...O	0.82	1.80 (3)	2.537(5)	148

Symmetry transformation used to generate equivalent atoms: (1) $1/2 - x, 1/2 + y, 1/2 - z$; (2) $1 - x, y, 1/2 - z$; (3) $x, 1 - y, -1/2 + z$; (4) $1 - x, y, 1/2 - z$; $1/2 - x, 1/2 + y, -z$.

H_2L^{-1} , one coordinated aqua molecule and one DMF molecule in the lattice Fig. 1(a).

The coordination mode of the ligand H_2L^{-1} is given in Fig. 1(b). The ligand binds the metal via the N atom of the pyridyl moiety and a different metal through the carboxylate O atom in monodentate fashion. The other carboxylate oxygen atom of the ligand remains uncoordinated. In coordination polymers **1–4**, each metal ion shows a distorted octahedral MN_2O_4 coordination environment, Fig. 1(c), with ligation from two monodentate carboxylate oxygen atoms of independent H_2L^{-1} ligands, two oxygen atoms from coordinated water molecules and two nitrogen atoms from two independent pyridyl moieties.

Therefore, efficiently packed 1D ladder-like double chain coordination polymers have been formed (Fig. 2a). The double-chain frameworks consist of two one-dimensional linear chains which extend in parallel pairs and are thus joined at the metal node in a ladder fashion. Two ligands adopt a certain configuration to connect two metal centers in such a way to form rectangular units (Fig. 2b). In each rectangular units the $\text{M} \cdots \text{M}$ distance is 11.70 Å. It is worth noting that the alternating rectangular planes are almost perpendicular to each other. Moreover, both the phenyl rings in each unit are no longer coplanar, but are twisted with a dihedral angle of 37.22° with respect to each other. All the metal coordinated N and O distances are within the normal ranges allowing for statistical errors [36]. The salient parameters of complexes **1–4** are summarized in Table 2.

The supramolecular frameworks are primarily stabilized by $\text{H} \cdots \text{O}$ interactions (2.529(5)–2.686(5) Å) originating from the H-atoms of coordinated water molecules and the O atoms of the lattice DMF molecules. Intramolecular H-bonding also exists between hydroxyl-H atoms with one of the free carboxylate oxygen atoms. Selected hydrogen bond distances (Å) and bond angles (°) in **1–4** are summarized in Table 3. Furthermore, there are $\text{C} \cdots \text{H} \cdots \text{O}$ short contacts between aromatic C–H groups of H_2L^{-1} units with the O

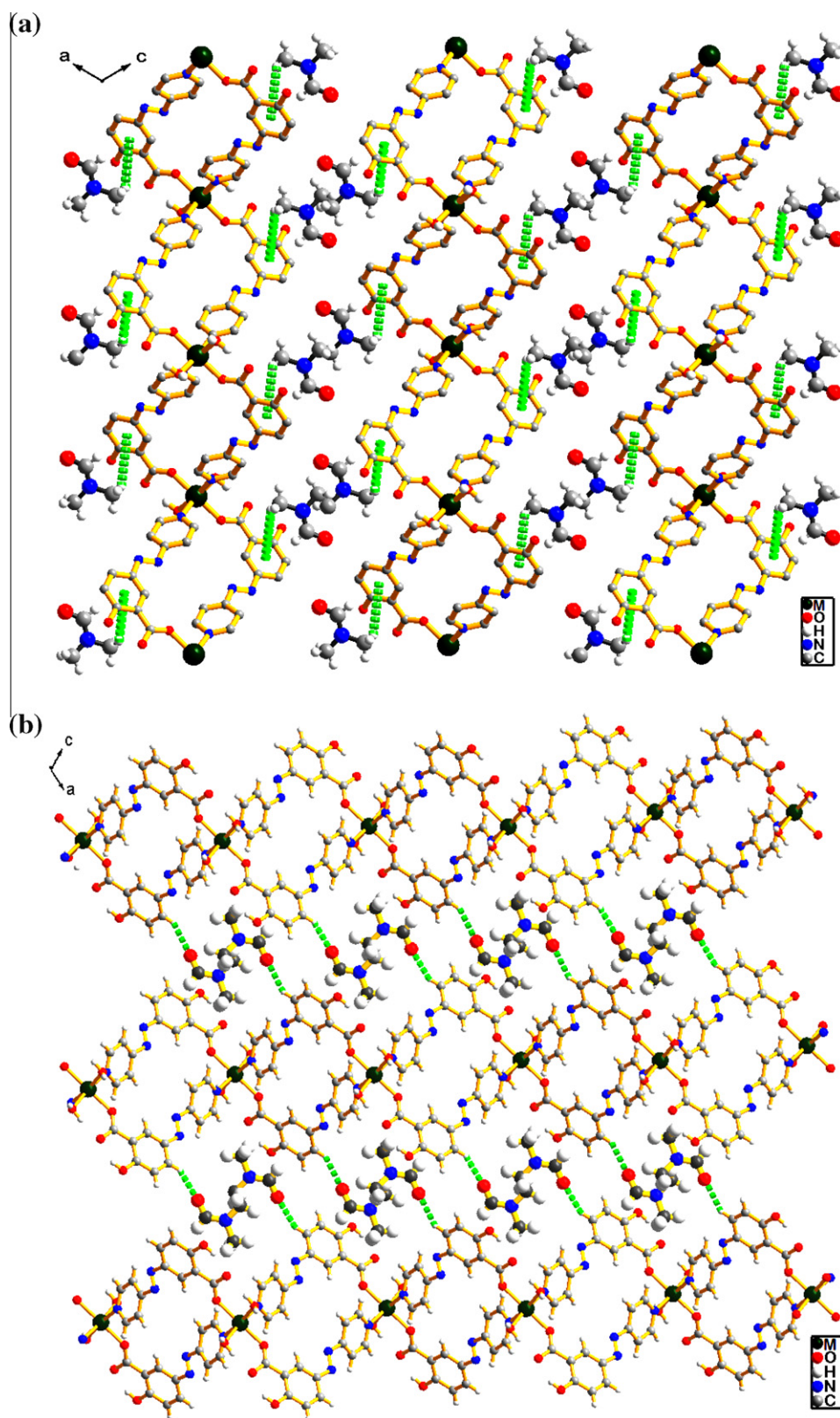


Fig. 3. 3D architecture showing (a) C–H... π interactions between the H atom of the methyl group of lattice DMF and the aromatic ring of the ligand H^+L^{-1} and (b) H-bonded structure.

atoms of neighboring coordinated water molecules, as well as with O atoms of the hydroxyl group of the ligand. The H atoms of the DMF molecules also show C–H... π interactions (2.860–2.870 Å)

with aromatic C–H groups (Fig. 3). Therefore the supramolecular structures of **1–4** involve weak C–H... π interactions between the H atoms of the methyl group of lattice DMF and the aromatic ring

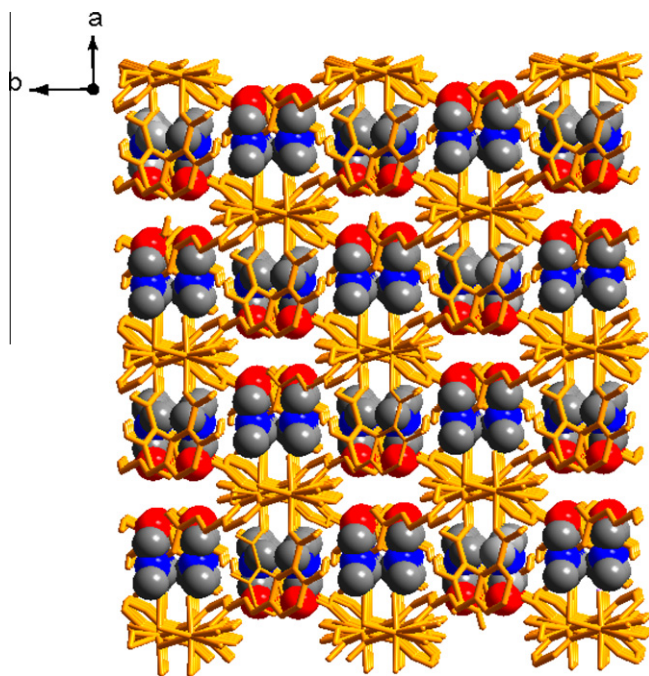


Fig. 4. 3D architecture showing embedded DMF molecules in a space-filled model.

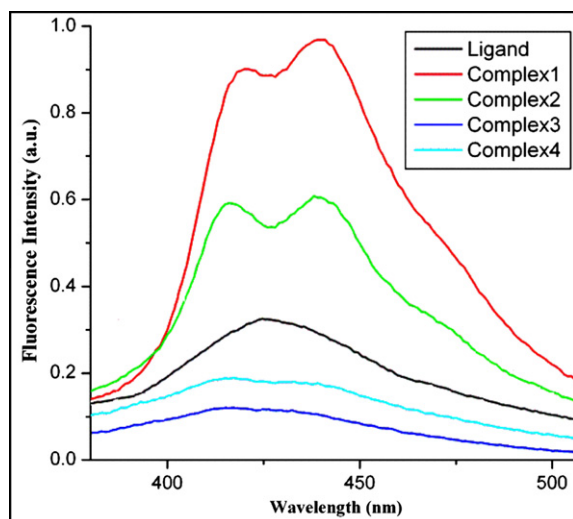


Fig. 5. Solid-state emission spectra at room temperature.

of the ligand H^+L^{-1} , which is further reinforced by strong non-covalent H-bonding interactions involving solvent molecules, to form an overall 3D structure (Fig. 4).

It is obvious from the descriptions that the behavior of the ligand and the reaction conditions have not shown any significant effects on the final architectures of the resulting complexes, hence resulting in the formation of the isostructural polymers. In addition, a non-symmetric ligand like H^+L^{-1} does not favor high dimensional supramolecular architectures, possibly due to its stabilization.

3.2. PXRD analysis

Powder X-ray diffraction (PXRD) patterns of complexes **1–4** are in agreement with the simulated patterns obtained from the single crystal X-ray data. It confirms that the crystal structures are truly

representative of the bulk phase. The observed differences in intensity could be due to the preferred orientation of the powder samples (Supplementary information, Figs. S9–S12).

3.3. Thermogravimetric analysis (TGA)

In order to examine the thermal stabilities of complexes **1–4**, thermal analyses were carried out in a N_2 atmosphere at the rate of 5°C per minute. ¹ Since all the coordination polymers are isostructural and have equal numbers of coordinated water and lattice DMF molecules, they exhibit a similar type of weight loss pattern in the thermograms. Complex **1** shows a weight loss of 24.65% (expected = 24.89%) within the temperature range $80\text{--}260^\circ\text{C}$ that corresponds to the release of both coordinated water and lattice DMF molecules. The framework is stable up to 400°C . Complex **2** exhibits a weight loss of 23.17% (expected = 23.39%) within the temperature range $80\text{--}230^\circ\text{C}$. The framework starts to decompose beyond 350°C . Similarly, complexes **3** and **4** shows a weight loss of 25.11% (expected = 25.25%) within the temperature range $80\text{--}230^\circ\text{C}$. Both frameworks are stable up to $\sim 380^\circ\text{C}$ (see Figs. S13–S16, Supporting information).

3.4. Photoluminescence studies

Fluorescent compounds are an immense current research area because of their diverse applications in chemical sensors, photochemistry, as well as electroluminescent displays [36–38]. Metal coordination compounds have been reported to exhibit the ability to tune the emission wavelength as well as the intensity of the free-organic compounds after coordination with metals. The photoluminescent properties of compounds **1–4** and the metal-free ligand H^+L^{-1} were investigated in the solid state at room temperature. The emission spectra of complexes **1–4** and the H^+L^{-1} ligand are depicted in Fig. 5. Upon excitation at 344 nm (Supporting information, S17), **1–4** show an unsymmetrical emission as a pair of bands at 438, 437, 431 and 435 nm and correspondingly other bands at 420, 417, 414 and 419 nm, respectively. However, the emission wavelengths at higher energy could be due to intra-ligand interactions as the profile of the emission band is quite similar to that of the free-ligand, while the low energy bands probably originate from ligand-to-metal charge transfer [39]. Compared with the ligand, complexes **1** and **2** exhibit enhanced luminescent intensity, while **3** and **4** show the opposite behavior. Usually, upon complexation with a metal center a degree of enhancement in photoluminescent intensities are observed as the metal center effectively increases the rigidity of the ligand and reduces the loss of energy by radiation-less decay [40]. In the case of complexes **3** and **4**, however, the quenching of the photoluminescent intensity has been observed due to presence of paramagnetic metal ions [41–44]. Therefore, the quenching of the luminescent emissions in **3** and **4** could be attributed to the σ -donation coordination environment of the Mn(II)/Co(II) ions, which result in the lowering of the energy gaps between two energy states. The metal...metal distances are long enough (more than 3.6 Å) to explain a cluster-centered transition caused by the metal...metal interactions in all the complexes.

4. Conclusion

In conclusion, we have described the construction of four new isostructural coordination polymers at room temperature. We have chosen an unsymmetrical azo-group containing organic ligand for the construction of coordination polymers with different transition metal ions. Solid-state luminescence of the complexes has been achieved at room temperature. We are in the process of synthesizing

similar type of ligands for constructing coordination polymers for various applications.

Acknowledgements

We gratefully acknowledge Prof. P.K. Bharadwaj for providing laboratory facilities. M.A thanks the CSIR for a SRF.

Appendix A. Supplementary data

CCDC 890674–890677 contains the supplementary crystallographic data for Compounds **1–4**. These data can be obtained free of charge via <http://www.ccdc.cam.ac.uk/conts/retrieving.html>, or from the Cambridge Crystallographic Data Centre, 12 Union Road, Cambridge CB2 1EZ, UK; fax: (+44) 1223 336 033; or e-mail: deposit@ccdc.cam.ac.uk. Supplementary data associated with this article can be found, in the online version, at <http://dx.doi.org/10.1016/j.poly.2013.02.044>.

References

- [1] M.K. Sharma, I. Senkovska, S. Kaskel, P.K. Bharadwaj, *Inorg. Chem.* 50 (2011) 539.
- [2] Z. Chang, D.-S. Zhang, T.-L. Hu, X.-H. Bu, *Cryst. Growth Des.* 11 (2011) 2050.
- [3] H. Furukawa, N. Ko, Y.B. Go, N. Aratani, S.B. Choi, E. Choi, A.O. Yazaydin, R.Q. Snurr, M. O'Keeffe, J. Kim, O.M. Yaghi, *Science* 329 (2010) 424.
- [4] R. Matsuda, R. Kitaura, S. Kitagawa, Y. Kubota, R.V. Belosludov, T.C. Kobayashi, H. Sakamoto, T. Chiba, M. Takata, Y. Kawazoe, Y. Mita, *Nature* 436 (2005) 238.
- [5] H.-S. Choi, M.P. Suh, *Angew. Chem., Int. Ed.* 48 (2009) 6865.
- [6] R.K. Das, A. Aijaz, M.K. Sharma, P. Lama, P.K. Bharadwaj, *Chem. A – Eur. J.* 18 (2012) 6866.
- [7] A. Karmakar, H.M. Titi, I. Goldberg, *Cryst. Growth Des.* 11 (2011) 2621.
- [8] L. Ma, C. Abney, W. Lin, *Chem. Soc. Rev.* 38 (2009) 1248.
- [9] T. Kundu, S.C. Sahoo, R. Banerjee, *Chem. Commun.* 48 (2012) 4998.
- [10] M. Ahmad, M.K. Sharma, R. Das, P. Poddar, P.K. Bharadwaj, *Cryst. Growth Des.* 12 (2012) 1571.
- [11] H. Miyasak, M. Julve, M. Yamashita, R. Clerac, *Inorg. Chem.* 48 (2009) 3420.
- [12] H.-L. Jiang, Q. Xu, *Chem. Commun.* 47 (2011) 3351.
- [13] K. Yaneda, M. Ohba, T. Singa, H. Oshio, S. Kitagawa, *Chem. Lett.* 36 (2007) 1184.
- [14] Y. Cui, Y. Yue, G. Qian, B. Chen, *Chem. Rev.* 112 (2012) 1126.
- [15] K.E. Knope, D.T. de Lill, C.E. Rowland, P.M. Cantos, A. de Bettencourt-Dias, C.L. Cahill, *Inorg. Chem.* 51 (2012) 201.
- [16] M.D. Aleenfort, C.A. Bauer, R.K. Bhakta, R.J.T. Houk, *Chem. Soc. Rev.* 38 (2009) 1330.
- [17] P. Harcajada, T. Chalati, C. Serre, B. Gillet, C. Sebrie, T. Baati, J.F. Eubank, D. Heurtaux, P. Clayette, C. Kreuz, J.-S. Chang, Y.K. Hwang, V. Marsaod, P.-N. Baries, L. Cynaber, S. Gil, G. Ferey, P. Couvreur, R. Gref, *Nat. Mat.* 9 (2010) 172.
- [18] H. Chun, H. Jung, J. Seo, *Inorg. Chem.* 48 (2009) 2043.
- [19] A.-W. Xu, C.-Y. Su, Z.-F. Zhang, Y.-P. Cai, C.-L. Chen, *New. J. Chem.* 25 (2001) 479.
- [20] H. Wang, L.-H. Huo, Z.-P. Deng, H. Zhao, S. Gao, *Cryst. Eng. Comm.* 14 (2012) 3501.
- [21] M.-S. Liu, Q.-Y. Yu, Y.-P. Cai, C.-Y. Su, X.-M. Lin, X.-X. Zhou, J.-W. Cai, *Cryst. Growth Des.* 8 (2008) 4083.
- [22] A. Aijaz, P. Lama, P.K. Bharadwaj, *Inorg. Chem.* 49 (2010) 5883.
- [23] O. Ohmori, M. Fujita, *Chem. Commun.* 14 (2004) 1586.
- [24] K. Koh, A.G.-F. Wong, A.J. Matzger, *Angew. Chem., Int. Ed.* 47 (2008) 677.
- [25] P. Lama, A. Aijaz, E.C. Sañudo, P.K. Bharadwaj, *Cryst. Growth Des.* 10 (2010) 283.
- [26] S.-S. Chen, Y. Zhao, J. Fan, T.-A. Okamura, Z.-S. Bai, Z.-H. Chen, W.-Y. Sun, *Cryst. Eng. Comm.* 14 (2012) 3564.
- [27] S.S. Nagarkar, A.K. Chaudhari, S.K. Ghosh, *Inorg. Chem.* 51 (2012) 572.
- [28] T.S. Basu, S. Dhar, S.M. Pyke, E.R.T. Tiekink, E. Rivarala, R. Batchner, F.E. Smith, *J. Organomet. Chem.* 633 (2001) 7.
- [29] *International Tables for X-Ray Crystallography*, vol. III, Kynoch Press, Birmingham, England, 1952.
- [30] SAINT, version 6.02, Bruker AXS, Madison, WI, 1999.
- [31] G.M. Sheldrick, SADABS, Empirical Absorption Correction Program, University of Göttingen, Göttingen, Germany, 1997.
- [32] XPREF, version 5.1, Siemens Industrial Automation Inc., Madison, WI, 1995.
- [33] G.M. Sheldrick, SHELXTL Reference Manual, Version 5.1, Bruker AXS, Madison, WI, 1997.
- [34] G.M. Sheldrick, SHELXL-97: Program for Crystal Structure Refinement, University of Göttingen, Göttingen, Germany, 1997.
- [35] D. Dobrzynska, L.B. Jerzykiewicz, J. Jezierska, M. Duczmal, *Cryst. Growth Des.* 5 (2005) 1945.
- [36] J.E. McGarrah, Y.J. Kim, M. Hissler, R. Eisenberg, *Inorg. Chem.* 40 (2001) 4510.
- [37] Q. Wu, M. Esteghamatian, N.X. Hu, Z. Popovic, G. Enright, Y. Tao, M. D'lorio, S. Wang, *Chem. Mater.* 12 (2000) 79.
- [38] M.D. Allendorf, C.A. Bauer, R.K. Bhakta, R.J.T. Houk, *Chem. Soc. Rev.* 38 (2009) 1330.
- [39] Y. Zhou, W.X. Mingyan, A. Lan, L. Zhang, R. Feng, F. Jiang, M. Hong, *Inorg. Chem. Commun.* 15 (2012) 140.
- [40] S.L. Zheng, J.H. Yang, X.L. Yu, X.M. Chen, W.T. Wong, *Inorg. Chem.* 43 (2004) 830.
- [41] H. Yersin, A. Vogler, *Photochemistry and Photophysics of Coordination Compounds*, Springer, Berlin, 1987.
- [42] B. Valeur, *Molecular Fluorescence: Principles and Application*, Wiley-VCH, Weinheim, 2002.
- [43] T.M. Muzioł, T. Lis, M. Barwiolek, E. Szlyk, *Dalton Trans.* 40 (2011) 11012.
- [44] R. Singh, M. Ahmad, P.K. Bharadwaj, *Cryst. Growth Des.* 12 (2012) 5025.